Final Report

Contract NASW 2967

Optical Fiber Waveguide Sagnac Interferometer Phase I: Multiturn One Meter Diameter, Single Mode

Submitted to:

National Aeronautics and Space Administration
Office of Aeronautics and Space Technology
Washington, D. C. 20546

Prepared by:

Victor Vali (Principal Investigator)
Richard W. Shorthill
Michael F. Berg

(NASA-CR-155574) OPTICAL FIBER WAVEGUIDE SAGNAC INTERFEROMETER. PHASE 1: MULTITURN ONE METER DIAMETER, SINGLE MODE Final Report (Utah Univ.) 29 p HC A03/MF A01 CSCL 20F G3/74
N78-16790
Unclas
15102

Submitted by:

Geospace Sciences Laboratory
University of Utah Research Institute
391 Chipeta Way, Suite D
Salt Lake City, Utah 84108

September 20, 1977

Geospace Sciences Laboratory Publication 77008

TABLE OF CONTENTS

1.0 BACKGROUND

1.1 Introduction

The purpose of this study was to build a rotating Sagnac interferometer using 100 meters of single mode fiber. It was planned to make the diameter one meter; however, because of other research being carried out at the Geospace Sciences Laboratory (GSL), it was possible to build the gyroscope 20 inches in diameter. The system, a Fiber Interferometer Gyroscope (FIG) was successfully built, tested, and demonstrated.

1.2 Sagnac Interferometer

When a Sagnac ring interferometer is rotated with angular velocity ω, the fringes shift by an amount given[1] by

$$\Delta Z = \frac{4\omega A}{\lambda c} \quad ,$$

where A is the area enclosed, λ is the wavelength of light, and c is the velocity of light. The time delay between the counter rotating beams and therefore, the fringe shift is increased by the factor of N when the light beams are made to travel around the area N times[2]:

$$\Delta Z = \frac{4\omega NA}{\lambda c} \quad .$$

When the beam path is used as a laser cavity (ring-laser) then,

$$\frac{\Delta f}{f} = \frac{\Delta \ell}{\ell}$$

where Δf is the beat frequency caused by the frequency difference between the counter rotating beams, and $\Delta \ell = \lambda \Delta Z$. Therefore, the beat frequency is (because when the laser cavity is wrapped around the area N times, its length is $N\ell$) given by,

$$\Delta f = f \frac{\Delta \ell}{\ell} = f \frac{4\omega NA}{cN\ell} = \frac{f\omega A}{c\ell} \quad .$$

ORIGINAL PAGE IS OF POOR QUALITY

This means that wrapping the laser cavity around an area N times does not increase the beat frequency (or sensitivity). The increase in the effective area is cancelled out by the increase in the cavity length.

2.0 CONCEPT

Sagnac interferometers have not been considered for guidance applications because of their lack of sensitivity as compared with the ring-lasers. The performance, however, can be considerably improved by circumscribing an area many times. In addition, the Sagnac interferometer has no dead band, which is a great advantage over the ring-lasers for certain applications (i.e., when ω is small).

(a) Ring Interferometer Gyroscope

The fringe shift ΔZ_s observed in a rotating ring (Sagnac) inteferometer is[2]

$$\Delta Z_s = \frac{4\omega A}{\lambda c}$$

where ω is the angular velocity of the system, A is the area enclosed by the counter rotating beams, λ is the wavelength of light and c is the velocity of light. If the area is circumscribed by the beams N times, the fringe shift is increased by factor of N,

$$\Delta Z_s = \frac{4\omega NA}{\lambda c}$$

The path is normally formed by a square with mirrors at each corner and a suitable beamsplitter arrangement.

(b) Fiber Interferometer Gyroscope

When an optical fiber waveguide is used as the beam path, it is made circular

$$A = \pi R^2 \quad ,$$

where R is the radius of the circle. Hence for a circle,

$$\Delta Z_s = \frac{4\omega N \pi R^2}{\lambda c} \quad *$$

$$= \frac{2\omega L R}{\lambda c}$$

$$= k_1 L \quad ,$$

where L is the length of the optical waveguide, and $k_1 = \frac{2\omega R}{\lambda c}$.

The photon noise limited minimum distance Δx that can be detected is[3],

$$\Delta x = \lambda\!\!\!^{-} \sqrt{B} \sqrt{\frac{h\nu}{\eta P}}$$

and where $\lambda\!\!\!^{-} = \frac{\lambda}{2\pi}$, B is the detector bandwidth, $h\nu$ is the energy per photon, η is the efficiency of the photodector and P is the beam power.

The corresponding minimum detectable fringe shift ΔZ_m is

$$\Delta Z_m = \frac{\Delta x}{\lambda} = \frac{\sqrt{B}}{2\pi} \sqrt{\frac{h\nu}{\eta P}}$$

ORIGINAL PAGE IS OF POOR QUALITY

$$= k_2 \frac{1}{\sqrt{P}}$$

where $k_2 = \frac{\sqrt{B}}{2\pi} \sqrt{\frac{h\nu}{\eta}}$.

* The fringe shift is almost solely determined by the free-space λ and c[2]. The dispersion term $(\frac{\lambda}{n} \frac{dn}{d\lambda})$ is small.

The signal to noise ratio is to be maximized, i.e.,

$$\frac{d}{dL}\left(\frac{\Delta Z_s}{\Delta Z_m}\right) = 0$$

$$\frac{d}{dL}\left(\frac{k_1 L}{k_2 \frac{1}{\sqrt{P}}}\right) = 0$$

But in an attenuating optical waveguide

$$P = P_o \, 10^{-aL}$$

where P_o is the initial power, P is the final power, and a is the attenuation coefficient. It is usually given in terms attenuation per kilometer, dB/km. Therefore,

$$\frac{\Delta Z_s}{\Delta Z_m} = \frac{k_1 L}{k_2} \sqrt{P_o \, 10^{-aL}}$$

$$= k_3 L \, 10^{-\frac{a}{2} L}$$

where $k_3 = \frac{k_1}{k_2} \sqrt{P_o}$.

Hence, to find the optimum length L,

$$\frac{d}{dL}\left(k_3 L \, 10^{-\frac{a}{2} L}\right) = 0 \quad ,$$

then,

$$k_3 \, 10^{-\frac{a}{2} L} - k_3 L \, (\ln 10) \, \frac{a}{2} \, 10^{-\frac{a}{2} L} = 0 \quad ,$$

thus,

$$1 = 2.3 \, L \, \frac{a}{2}$$

Therefore, the optimum length L of the optical waveguide is given by,

$$L = 0.87 \, \frac{1}{a} \quad .$$

In the case of a waveguide with 2 dB/km attenuation the maximum length L is

$$L = 0.87 \, \frac{1}{0.2}$$

$$= 4.3 \text{ km}$$

(for a = 20 db/km, L = 0.43 km)

A 3 milliwatt laser emits 10^{16} photons/sec. This will be attenuated to 0.5 milliwatts by the 4.3 km long 2 dB/km waveguide. The corresponding noise amplitude ΔZ_n is then,

$$\Delta Z_n = \frac{\sqrt{B}}{2\pi} \sqrt{\frac{h\nu}{\eta P}}$$

ORIGINAL PAGE IS OF POOR QUALITY

$$= \frac{\sqrt{B}}{2\pi} \cdot \frac{1}{\sqrt{M}}$$

where M is the number of photons detected per second. For the detected, 0.5 milliwatts $M = 2 \cdot 10^{15}$ photons/sec. The detector bandwidth B (or reciprocal response time) is taken to be 10 Hz (0.1 seconds response time).

Therefore, the noise amplitude in terms of fringe shift is

$$\Delta Z_n = \frac{3}{2\pi} \frac{1}{\sqrt{2 \cdot 10^{15}}}$$

$$\simeq 10^{-8} \text{ fringes} \quad .$$

This is equal to the minimum detectable signal ΔZ_m that is,

$$\Delta Z_m = \frac{2\omega LR}{\lambda c} = \Delta Z_n$$

Hence, the minimum detectable angular velocity ω_{min} is

$$\omega_{min} = \frac{\Delta Z_m \lambda c}{2LR}$$

Here $L = 4.3 \cdot 10^5$ cm and $R = 15$ cm thus in this example

$$\omega_{min} = \frac{10^{-8} \cdot 6 \cdot 10^{-5} \cdot 3 \cdot 10^{10}}{2 \cdot 4.3 \cdot 10^5 \cdot 15}$$

$$\simeq 1.4 \cdot 10^{-9} \text{ rad/sec} \quad .$$

Compared with the rotation velocity of the earth

$\omega_{earth} = 7 \cdot 10^{-5}$ rad/sec

$$\frac{\omega_{min}}{\omega_{earth}} = \frac{1.4 \cdot 10^{-9}}{7 \cdot 10^{-5}}$$

$$= 2 \cdot 10^{-5}$$

3.0 PREVIOUS STUDIES

The previous investigations carried out by the GSL include:

1. Air path Sagnac Interferometer.
2. Multimode Fiber Experiments
   (a) 50 meter Mach-Zender Interferomter
   (b) 50 meter Sagnac Interferometer
3. Singlemode-Fiber Experiments
   (a) 10 Meter Mach-Zender Interferometer
   (b) 10 Meter Sagnac Interferometer
   (c) Optical fiber considerations
4. Ring Interferometer Experiments
   (a) One kilometer fiber
   (b) Single axis gyroscope - Fresnel-Fizeau drag experiment (100 meters)
5. Ring-Laser Experiments (Proprietary)

Although these experiments were not funded by the contract NASW 2967, they have provided the background leading to the current results reported here. These experiments have been carried out over a period of three years.

4.0 EXPERIMENTAL PLAN

4.1 Introduction

The original plan will be described below. The actual plan followed will also be detailed. Because of the delay in obtaining the funding for this research, other research results could be applied to the planning and Phase I and II were combined. The result was an accelerated research schedule.

4.2 Original Plan

The proposed program was a continuation of the previous experiments as described in 3.0. Therefore, it was planned for use of a single mode fiber in an experimental set-up to allow one to evaluate the instruments' sensitivity. The fiber waveguide Sagnac interferomter was to be placed on a rotating optical bench. It was not planned to reach the ultimate sensitivity with this version of the gyroscope. Therefore, only 100 meters of the fiber was to be used.

Figures 4.2-1 and 4.2-2 show the arrangement of optical and mechanical components for the Phase I study. The fiber was to be wound on a one meter diameter quartz cylinder. The large D is chosen to have a high sensitivity, since the fringe shift is

$$\Delta Z = \frac{\omega L D}{\lambda c}$$

At no place is the radius of curvature of the fiber less than 10 cm. Therefore, the curvature losses of light from the fiber are negligible(6). Numerically, for ω = 1 rad/sec, $L = 10^4$ cm, D = 100 cm, $\lambda = 6 \cdot 10^{-5}$ cm and $c = 3 \cdot 10^{10}$ cm/sec, the expected fringe shift is

$$\Delta Z \approx 0.5 \text{ fringes}$$

The Corning Glass Works has developed a single mode fiber for λ = 6328Å and was to be used. At present, this fiber has the attenuation coefficient α = 20 dB/km. The core of the fiber is 11 microns in diameter; however, making it easier to couple the light into it(4,5).

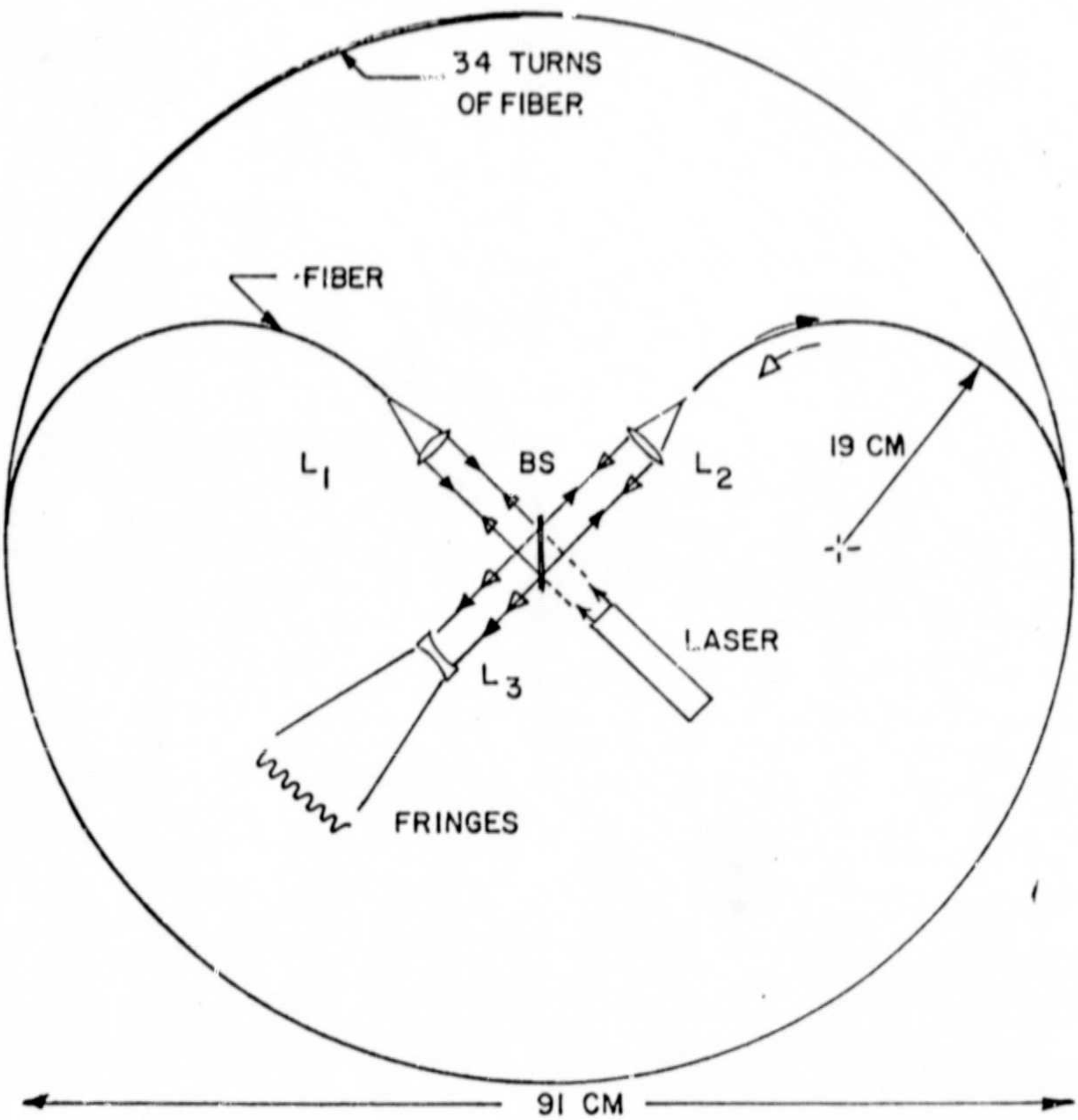

ORIGINAL PAGE IS
OF POOR QUALITY

Figure 4.2-1. Optical path for "Phase I: Multiturn One Meter Diameter Single Mode" Sagnac Interferometer

CAPTIONS FOR FIGURE 4.2-1

L_1	Converging lense fl 50 mm, dia 25 mm anti-reflection coated
L_2	Converging lense fl 50 mm, dia 25 mm anti-reflection coated
L_3	Diverging lense fl 50 mm, dia 50 mm anti-reflection coated
BS	Beamsplitter 50/50
Laser:	SP138 or equivalent
Fiber:	Single mode 34 turns, 100 meters long

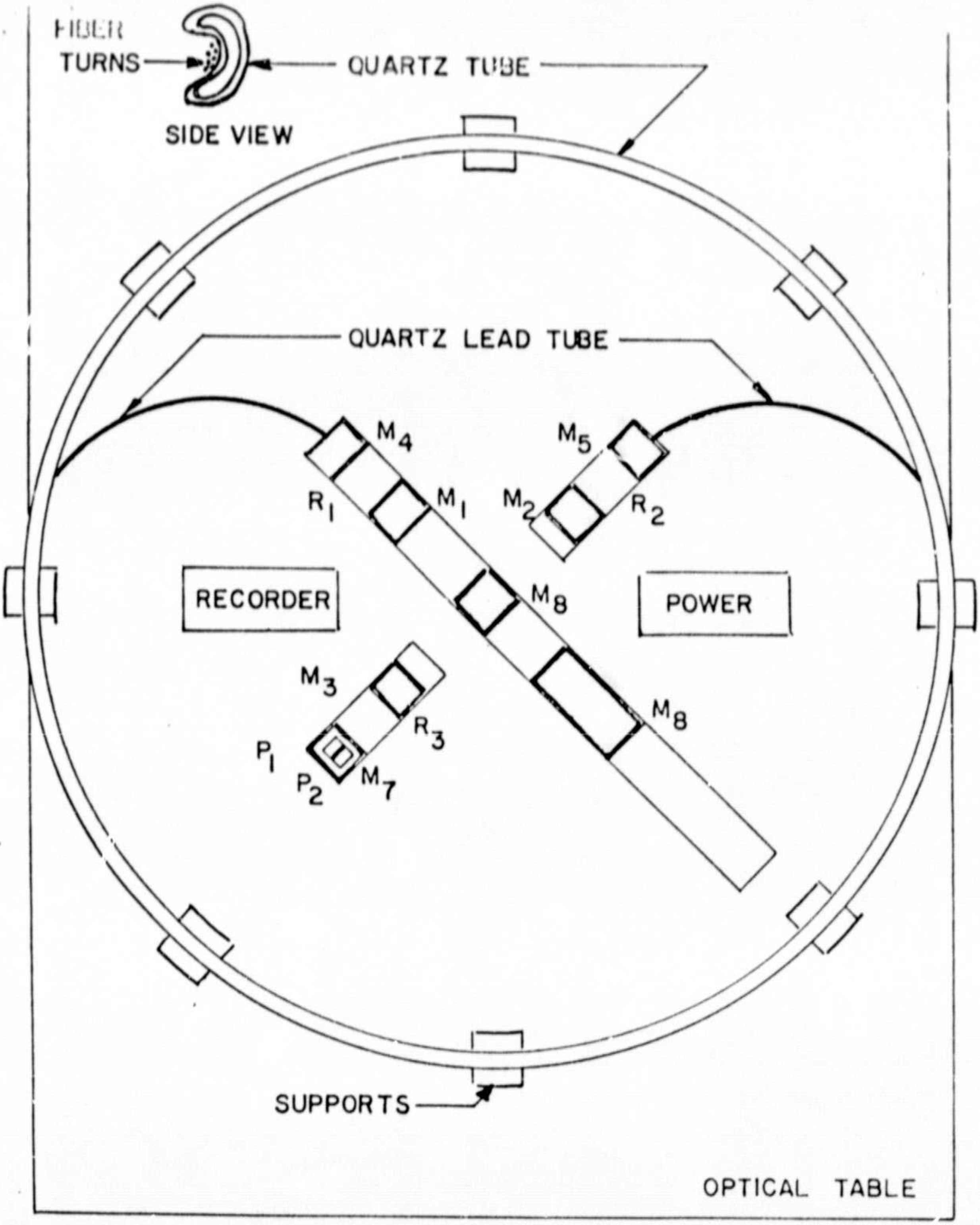

ORIGINAL PAGE IS
OF POOR QUALITY

Figure 4.2-2. Mechanical and Electrical Arrangment for "Phase I" study

CAPTIONS FOR FIGURE 4.2-2

M_1: X,Y motion, vertical feed rod, precision mirror mount, universal carrier, rod holder

M_2: X,Y motion, vertical feed rod, precision mirror mount, universal carrier, rod holder

M_3: Rod mounted carrier, vertical feed rod, bar type lens holder

M_4: X,Y,Z motion, precision mirror mount, universal carrier

M_5: X,Y,Z motion, precision mirror mount, universal carrier

M_6: 2 rod mount carrier, 2 adj dia optic holder, 2 bench rods

M_7: Cross feed carrier, vertical feed rod, bar type lens holder, dual uni-slide

M_8: Cross feed carrier, vertical feed rod, precision mirror mount

R_1: Precision table rail 24-inch

R_2: Precision table rail 6-inch

R_3: Precision table rail 6-inch

P_1: Photodetector

P_2: Photodetector

Optical Table 3x4 feet

Quartz Tube 3 meter formed into circle and collapsed

Quartz Lead Tube 60 cm each formed into semicircle

Power for Laser, Photodetectors and Recorder

Recorder, multichannel

The aim of this phase of the study was to obtain the experimental fringe shifts as a function of ω the angular velocity. Also, it was planned to find the best configuration of the optcial component to maximize the amount of light entering the fiber[4,5] and to minimize the effects of temperature variations and mechanical vibrations. The Original Plan is shown in Table 4.2-1. Note that the original work was to start September 1976.

The efforts in Phase II (which was to follow the successful completion of Phase I) would be directed toward improving the sensitivity of the gyroscope. This involves increasing the length of the fiber to at least 1 km and minimizing the fiber attenuation coefficient[7]. Also electronic read-out systems will be built that approaches the photon noise limit. Figure 4.2-3 represents the plan to be followed.

The efforts in Phase III (to follow the successful completion of Phase II) would be directed toward maximizing the sensitivity of the gyroscope. The optimum length of the fiber would be considered (e.g., 4.3 km for a 2 dB/km fiber). The size of the instrument would be chosen such that it can be developed into a flight test instrument.

TABLE 4.2-1 Schedule of Activities (Original Plan)

	ACTIVITY	Months from start 1	2	3	4	5	6	7
1	Order fiber	------Δ						
2	Order optical parts	------Δ						
3	Plan shop work, electronic design	------Δ						
4	Start construction of base		------	------	------Δ			
5	Preliminary testing: (1) ΔZ as a function of			------	------	------	---Δ	
6	(2) Optimum fringe configuration			------	------	------	---Δ	
7	(3) Optimum coupling conditions				------	------	---Δ	
8	(4) Rigidity					------	---Δ	
9	(5) Temperature sensitivity					------	---Δ	
10	(6) Laser requirements					------	---Δ	
11	Final report						------Δ	
12	Scientific paper						---	---Δ
13	Consult with JPL/CIT	Δ		Δ		Δ		
	START 9-28-76 END 3-20-77	OCT	NOV	DEC	JAN	FEB	MAR	

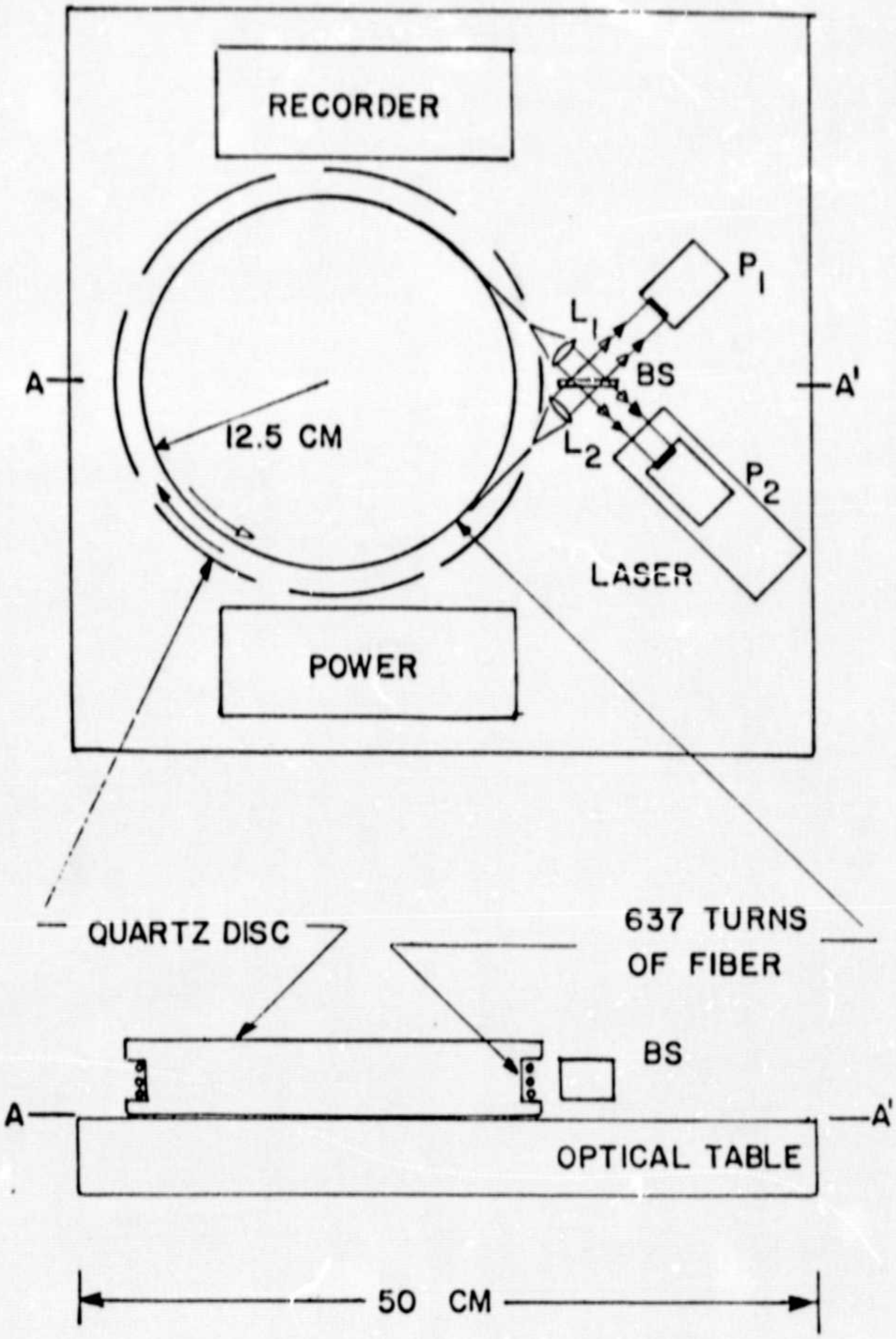

Figure 4.2-3. Component arrangement for "Phase II: Breadboard Gyroscope"

4.3 Actual Work

The actual work started September 28, 1976 and ended about September 20, 1977. There was a delay in obtaining the 100 meters of optical fiber. Advances in other fiber optics research being done in this Laboratory necessitated a change in schedule. A no-cost extension was obtained.

Several fiber suppliers were asked for quotes: (1) Corning Glass Works, Corning, N.Y., made the decision not to manufacture single mode fibers until some unspecified time in the future. The Corning fiber that we used previously was completely satisfactory, but we had only 10 meters, (2) Valtec Corporation, West Boylston, MA, just recently made some single mode fiber. We obtained a sample (about a meter) to test. It was not adequate for our purpose, (3) Fiber Communications Inc., Orange, N.H., have made single mode fiber. We obtained 100 meters but the attenuation was too large to be useful. It was returned for another 100 meters which had better attenuation characteristics, (4) International Tel. and Tel. (ITT), Roanoke, VA, has recently made some single mode fiber with very small attenuation. A sample was obtained and tested and 100 meters ordered.

A 1000 meter length of Corning single mode fiber was made for the Naval Electronics Laboratory Center, now Naval Ocean Systems Center. We have a contract with the Office of Naval Research to use this fiber to detect earth rotation. This we considered a "check-out" for the NASA study. The fiber was wound on a 40 cm tube 15 cm long. The results of this ONR experiment showed apparently that earth rotation could be detected as the coil was tilted in the NS direction. The experiment was repeated at our Laboratory with 100 meters of FCI fiber borrowed from Bill Goss/JPL because our 100 meters of FCI fiber had not arrived. Figure 4.3-1 shows the experimental set-up.

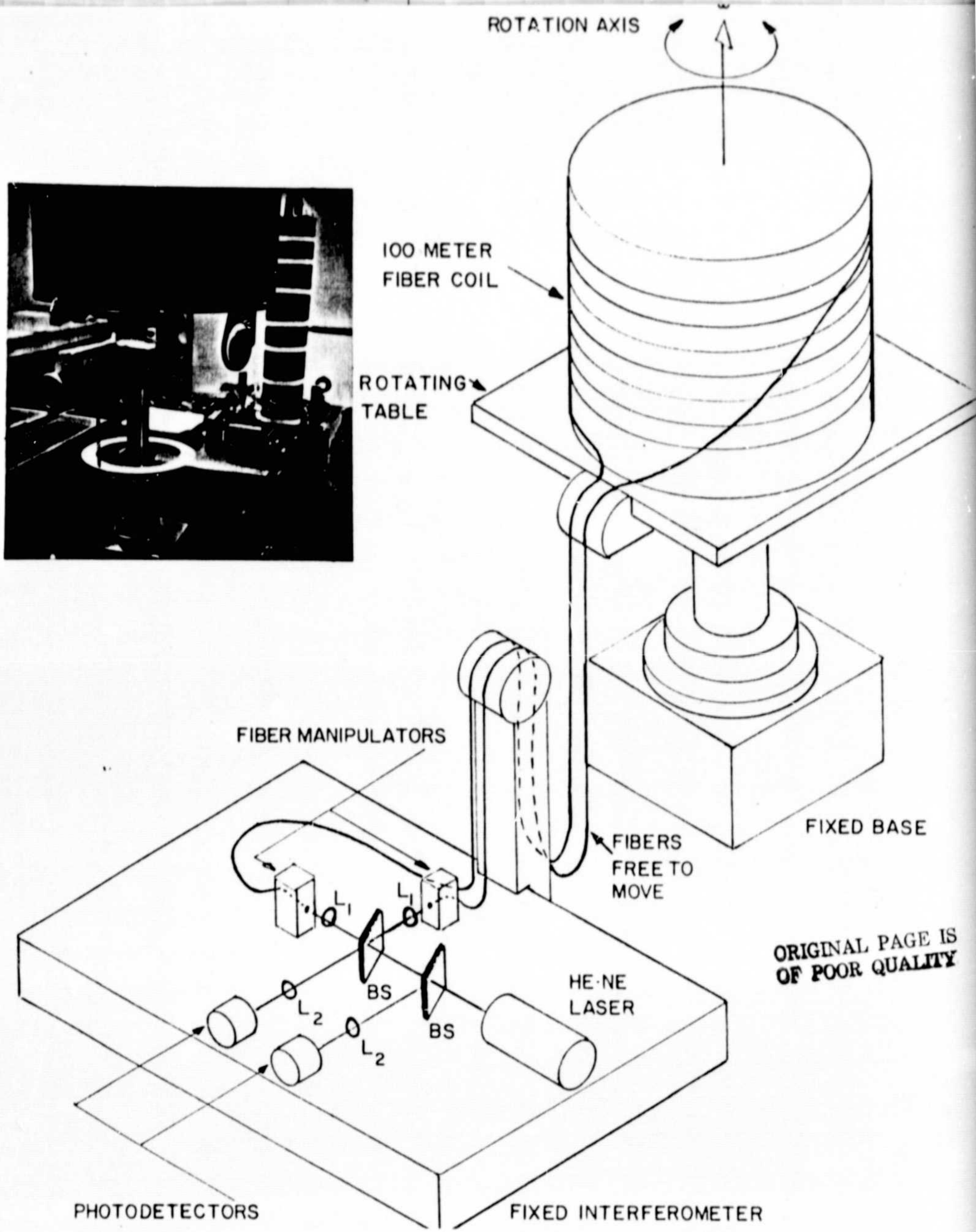

ORIGINAL PAGE IS
OF POOR QUALITY

Figure 4.3-1. Tilt table arrangement for detecting earth rotation with 100 meters of single mode fiber.

Thus, the NASA work was delayed because of the unavailability of single mode fiber as previously explained. The advantage of this delay is that optimizing of coupling light into the fiber was accomplished. A better fiber (ITT) was used to do the NASA study. In addition, Phase II could now be attempted in part.

The activities completed to March 31, 1977 (see Table 4.2-1) were: (1) fiber ordered, ITT single mode (4-5 μm core, 70 cm cladding, 15 dB/km attenuation at 850 nm, RTV coating with Teflon plastic covering, 100 m long, ~1% concentricity of core; (2) Most optical parts ordered or on hand; (3) Shop work started by our engineer. Electronic design, same as used in the ONR experiment; (4) The base construction not started; (5) Not started; (6) Optimum fringe configuration chosen; (7) Optimum coupling configuration chosen; (8) Not yet tested; (9) Not yet tested; (10) Laser a HeNe (gas); (11) Not started; (12) Not started; (13) Several consulting visits have been made between the University of Utah Research Institute and JPL. These visits were fruitful. It was estimated that the study was about 50% complete.

The work plan is shown in Table 4.3-1. The final result should be a coil 20 inch diameter and 8 to 10 inches high. This Fiber Interferometer gyroscope (FIG) was made portable so it can be demonstrated at various locations. Figure 4.3-2 shows a photograph of the actual configuration. Note the differences from the original are a smaller diameter ring, smaller elctronics, and smaller manipulators. This improved version was possible because we had an NSF and an ONR contract to do fiber research which, along with the NASA fiber research, permitted the sharing of the cost to solve mutual problems. The government has benefited because of this initial sharing of efforts and results.

TABLE 4.3-1. Schedule of Activities (New Plan)

	ACTIVITY	Extension	Months from start					
		APR	MAY	JUNE	JULY	AUG	SEPT	OCT
1	Test new ITT fiber		-------	-------Δ				
2	Order remaining optical parts	-------	-------Δ					
3	Modify ONR electronic design for this instrument		-------	-------Δ				
4	Complete design for base plate and mounting	-------Δ						
5	Assemble instrument				-------Δ			
6	Test instrument				----	-------Δ		
7	Write final report						--Δ	
8	Submit final report						Δ	
9	Consult with JPL	Δ		Δ		Δ		
10	Obtain a 6 month no cost extension	Δ						

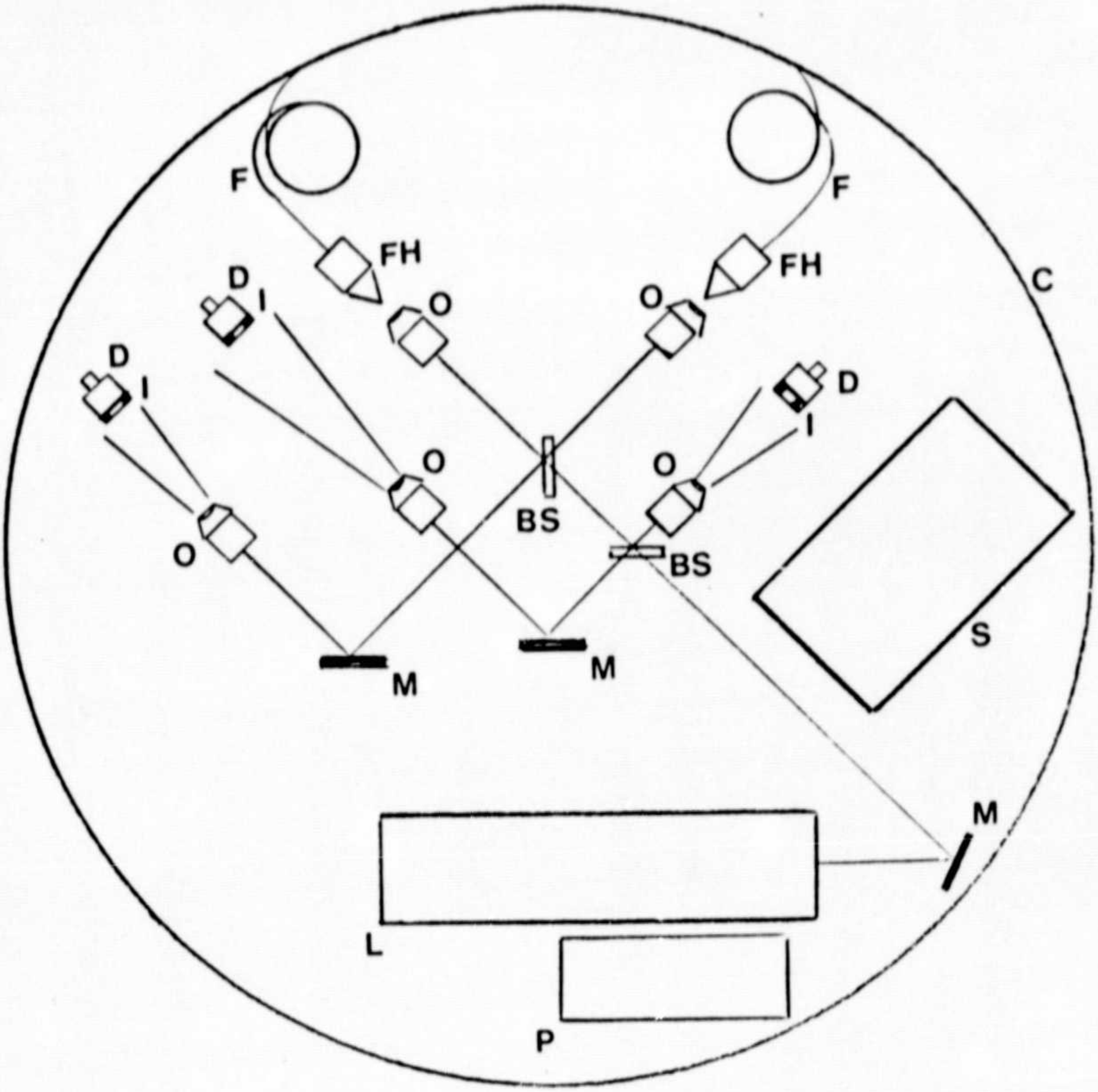

Figure 4.3-2. Diagram of Phase II interferometer (New Plan)
Where F = fiber, FH = fiber holder, C = fiber coil, D = detector, I = iris, BS = Beamsplitter, M = Mirror, L = Laser, P = power, S = signal conditioner, O = microscope objective.

5.0 RESULTS OF PHASE I AND II STUDY

5.1 Introduction

The following section describes some of the significant results of this study. It was shown that the FIG performed as expected; a fringe shift accuracy of 10^{-2} was obtained. The feasibility and potential of a FIG was demonstrated. The instrument showed the presence of certain noise sources, optical, mechanical, and thermal. Most important, however, the study demonstrated that further development is a prudent and reasonablc undertaking.

5.2 Fiber

The fibers from four suppliers were evaluated to various degrees. The ITT fiber currently holds the most promise because, among other things, it has low attenuation, good polarization characteristics, is single mode at 633 nm and at 850 nm and is easy to handle. The other fibers, Valtec and FCI, show potential also. The big problem with most fiber manufacturers is that they supply only the value of attenuation and physical dimensions. This is because for additional information, special instrumentation is required. For example, the fibers must be evaluated in the FIG configuration to evaluate the polarization properties.

A noise source is scattering. Inserting light into the core requires precise alignment of the optics and fiber (to less than 1 micrometer). The fiber ends must be flat. The angle of the end surface with the fiber axis can be varied by several methods but the fiber end must be flat at whatever angle used.

5.3 Temperature Effects

The Sagnac interferometer is inherently temperature insensitive to the first order because both rotating light beams pass through the same path. A change in fiber length is the same for both directions. Second order effects become important when improved accuracy is required.

5.4 Noise

The major source of noise was reflections from the fiber ends. This results in extraneous fringe patterns. These fringe patterns are temperature sensitive because the beam paths are not reciprocal.

Another noise source is scattering. This, however, requires investigation in the next study phase.

Another source of noise in the FIG design was mechanical. The optical components used to manipulate the mirrors, microscope objectives and fibers were not as rigid as desired. This was partly as result of the requirement to provide a device that could be demonstrated. The fiber manipulators were 5-axis devices. The required accuracy of adjustments was better than a micron which made the precise setting difficult. Cost was a factor in the design so that wherever possible, shelf items were used. Size was another factor, the small size (~50 cm diameter) limited the choice of shelf items. A smaller size (~20 cm diameter) would have been more rigid because it would be necessary to custom build all parts (with a resultant increase in cost).

Electronic noise was a minor consideration for the FIG and no attempt was made to optimize the detector, amplifier and display. A visual display of the fringes was found to be adequate for most purposes.

5.5 Accuracy

The overall accuracy of the FIG is shown in Figure 5.5-1. This is a laboratory worksheet. The sine wave shows a maximum fringe shift $\Delta Z = 2$. The vertical line indicates $\omega = 0$. The fringe shift can be measured to an accuracy of 10^{-2}. When these three major noise sources (reflections, scattering, and mechanical motion) are eliminated, it is estimated that the FIG (50 cm diameter, 85 meters of fiber, etc.) would obtain an accuracy of 10^{-4} of a fringe.

5.6 Laser Sources

Originally, it was planned to use a diode laser which emits at 850 nm. Because this radiation is not visible, a HeNe laser (633 nm) was used. There were problems with feedback into the laser. This feedback combined with the inherent instability of the inexpensive HeNe laser aggravated the stability even further. This added noise was, however, not large enough to prevent the planned operation (demonstration).

5.7 Optics and Electronics

The optical components used throughout the FIG were all standard shelf items. The mirrors were standard (1/10 λ, 1 inch dia., broadband 99% reflecting at 45°). The microscope objectives were 10X and 20X. The fiber manipulators were 5-axis systems ($X, Y, Z, \theta_X, \theta_Y$). A pin vise was used to hold the fiber and fit to the manipulators. The optics, holders, and mani-

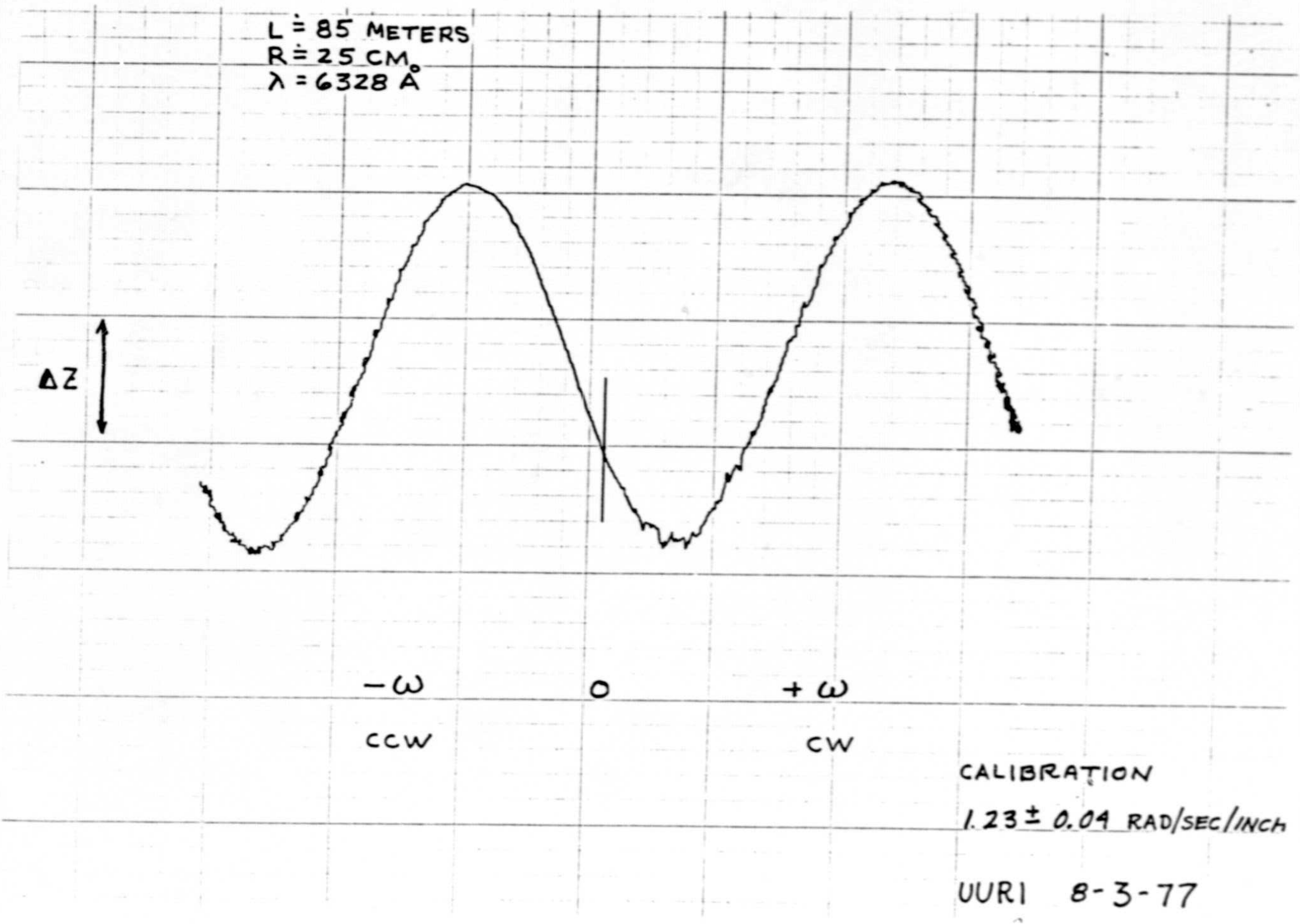

Figure 5.5-1. Test data for FIG.

pulators were obtained from Newport Research Corporation, Fountain Valley, Ca. The photodetectors were UDT-PIN 10DP. Operational amplifiers were used. An X-Y recorder was used to display the fringe shift. The FIG was placed on a simple rate table with an angular position and angular rate output signal. A small amount of mechanical noise was generated by the rate table.

5.8 Demonstrations

On October 5, 1977, testimony was given by Dr. James J. Kramer (Acting) Associate Administrator for Aeronautics and Space Technology, to the Subcommittee on Space Science and Applications Committee on Science and Technology House of Representatives.

Previously, two meetings were held at NASA-OAST where the results of the FIG study were presented and the FIG was demonstrated. In addition, the system was demonstrated at JPL earlier.

6.0 PHASE III STUDY

The Phase I study was completed; fringe shifts as a function of angular velocity were obtained, the configuration was optimized to maximize the light entering the fiber. Phase II, although not part of the initial plan, was partially completed. That is, the size was reduced from the one meter diameter to 50 cm diameter and the primary noise sources were identified.

The next research that should be started is the elimination of the noise sources already identified. Also a Fiber Ring Optical Gyroscope (FROG) using one kilometer of fiber should be built to identify the noise sources below the level of these three mentioned in previous sections.

Following this Phase III Study, a field instrument could be built; however, the 4.3 kilometer length suggested may not be appropriate. The attenuation of 2 dB/km requirement may not be obtainable for one to two years.

7.0 SUMMARY OF RESULTS

The Fiber Interferometer Gyroscope (FIG) was successfully completed and all objectives obtained. In addition, the second phase was in part completed. The major noise sources of noise were identified (reflections from the fiber ends, lack of mechanical rigidity, and possibly scattering). The accuracy, 10^{-2} of a fringe was obtained. It is estimated that by removing the major noise sources that the accuracy of 10^{-4} could be obtained with the present configuration. The required improvements for the next phase were determined such as fiber requirements, light source, read-out, etc. Finally, a visual summary is Figure 7.0-1 which shows the FIG instrument.

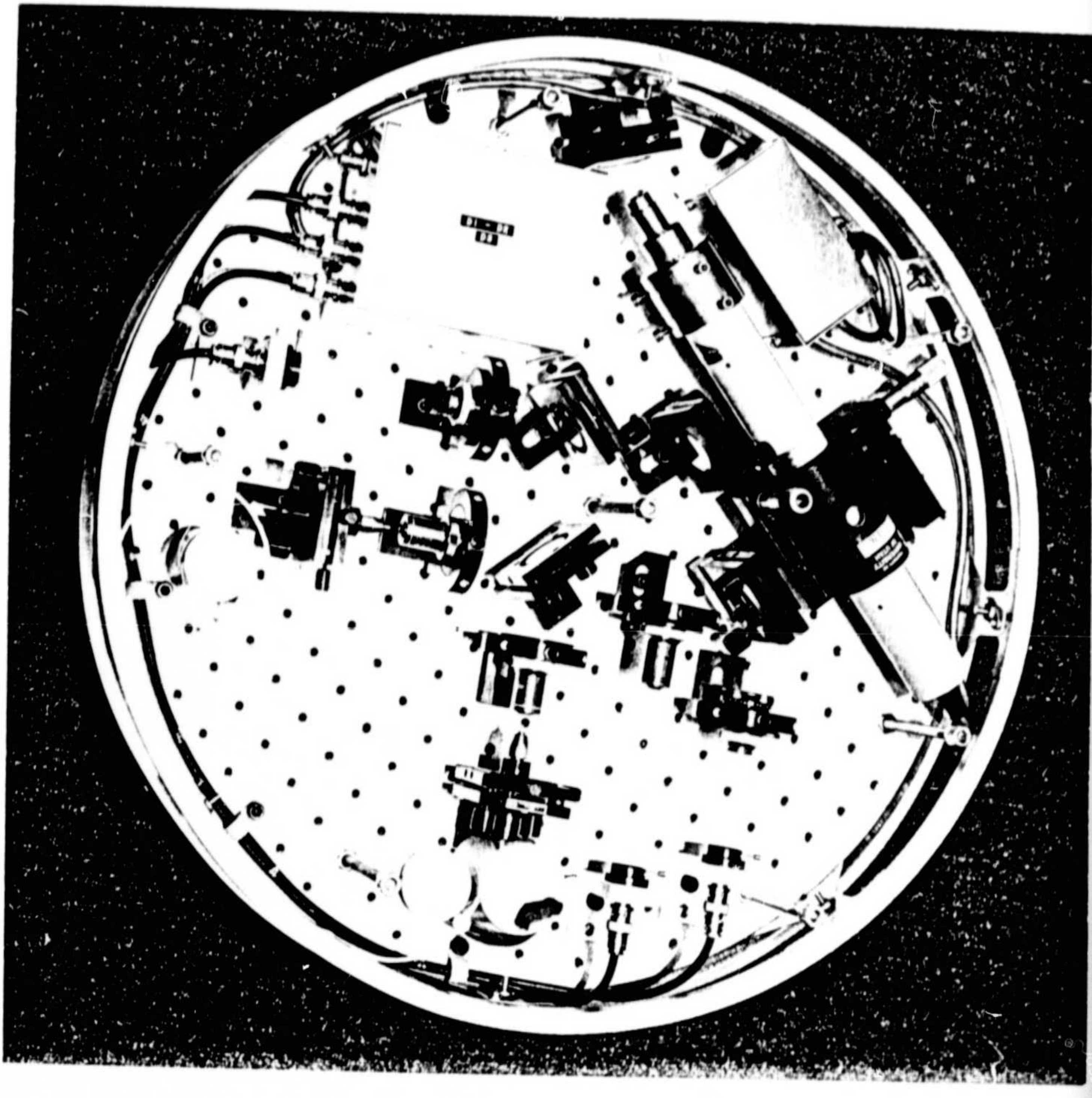

ORIGINAL PAGE IS
OF POOR QUALITY

Figure 7.0-1. Photograph of the Fiber Interferometer Gyroscope

8.0 REFERENCES

1) G. Joos, Theoretical Physics, 2nd Edition, Hafner Publishing Co. (1950) p. 471.

2) E. J. Post, Rev. of Modern Physics, Vol. 39, No. 2, April 1967, p. 475.

3) G. E. Moss, L. R. Miller and R. L. Forward, Applied Optics, Vol. 10, No. 11, November, 1971, p. 2495.

4) M. Imai and E. H Hara, Applied Optics, Vol. 13, No. 8, August, 1974, p. 1893.

5) M. Imai and E. H. Hara, Applied Optics, Vol. 14, No. 1, January, 1975, p. 169.

6) E. P. Kapron, D. B. Keck and R. D. Maurer, Appl. Phys. Lett., Volume 17, November 15, 1970, p. 423.

7) D. B. Keck, R. D. Maurer and C. P. Schultz, Appl. Phys. Lett., Volume 22, April 1, 1973, p. 307.